

# Design and Real-Time Implementation of Robust FACTS Controller for Damping Inter-Area Oscillation

Rajat Majumder, *Student Member, IEEE*, Bikash C. Pal, *Senior Member, IEEE*, Christian Dufour, *Member, IEEE*, and Petr Korba

**Abstract**—An application of a normalized  $\mathcal{H}_\infty$  loop-shaping technique for design and simplification of damping controllers in the liner matrix inequalities (LMI) framework is illustrated in this paper. The solution is sought numerically using LMIs with additional pole-placement constraints. This ensures that the time-domain specifications are met besides robust stabilization. The designed control algorithm is implemented using a rapid prototyping controller. The performance of the controller is validated in real time using a detailed model of the power system implemented using Linux PC-based, multi-processor technology. The coupling between the controller and the power system is through a set of DAC and ADC modules in the analogue domain.

**Index Terms**—Flexible ac transmission systems (FACTS),  $\mathcal{H}_\infty$  control, inter-area oscillations, LMIs, loop-shaping, normalized coprime factors, real-time implementation.

## I. INTRODUCTION

**D**AMPING of inter-area oscillations is one of the major challenges to the electric power system operators [1]. These oscillations are the manifestation of consequences of small disturbances in weakly interconnected power system. With ever-increasing power exchange between utilities over the existing transmission network in the open power trading regimes, the problem has become even more challenging. The secure operation of the system thus requires application of robust controllers to damp these inter-area oscillations. flexible ac transmission systems (FACTS) [2] devices installed in the system for dynamic voltage support and enhanced power flow can help the situation if equipped with a properly designed damping controller [3], [4].

The objective of control design exercise is to ensure adequate damping under all credible operating conditions. Recently, many researchers have investigated the use of  $\mathcal{H}_\infty$  optimization [5]–[7] and  $\mu$ -synthesis [8], [9] for power system robust damping control design. The concept of loop-shaping design was proposed by McFarlane and Glover [10]–[12]. It combines the characteristics of both classical open-loop shaping and the  $\mathcal{H}_\infty$  optimization. Zhu *et al.* [13] and Farsangi *et al.* [14]

have applied this technique for damping power oscillations. However, the problem was solved analytically using standard normalized coprime factorization approach, wherein the time-domain specifications in terms of minimum damping ratios (pole-placement) could not be considered explicitly in the design stage. Although the analytic procedure has a noniterative solution, the design requirements can only be captured through proper selection of weights, which is not always straightforward.

In this paper, the problem of robust stabilization of a normalized coprime factor plant description has been converted into a generalized  $\mathcal{H}_\infty$  problem [15]. The problem is solved using liner matrix inequalities (LMIs) [16]–[18] with additional pole-placement constraints. In addition to robust stabilization of the shaped plant, a minimum damping ratio could thus be ensured for the critical inter-area modes.

Usually the damping controller obtained from norm minimization-based design is quite complex in structure. Unlike the controller obtained from classical techniques, a controller designed using  $\mathcal{H}_\infty$  optimization offers greater challenge in implementation. The objectives of the research in this paper are design, implementation, and performance validation of such control in real time. One concern, however, is the availability of the actual system for validating the performance of the controllers in real time. It is extremely difficult to build even a prototype of an actual power system in the laboratory or in an equipment manufacturing test facility. For obvious reasons, it is rarely allowed to perform such validation tests in the field. From technical as well as commercial considerations, it is thus desirable to have a dynamic system emulator that can physically emulate the dynamic behavior of the power system in real time. Studies reported in [3], [4], [8], and [9] described simulation results. The implementation and experimental verification of a robust FACTS controller is described in this paper. The dynamic behavior of the power system is emulated in a real-time station (RTS) on which designed control algorithm is tested using a rapid prototyping controller (RPC). The hardware interface between the two platforms is in analogue domain through DAC/ADC modules, so that it is virtually impossible for the controller to distinguish between the actual plant and the emulated plant. Thus, the costly proposition of building a large prototype power system in the laboratory for testing purpose can be avoided.

This paper is organized as follows. Following this introductory section, the control design approach is briefly outlined in general sense in Section II. A case study with a prototype power system model is illustrated in Sections III and IV with controller performance in the frequency domain. The same controller is

Manuscript received September 20, 2005; revised January 16, 2006. This work was supported in part by EPSRC, U.K., under Grant GR/S06158/01 and in part by ABB Corporate Research Center, Switzerland.

R. Majumder and B. C. Pal are with the Department of Electrical and Electronic Engineering, Imperial College London, London SW7 2BT, U.K. (e-mail: r.majumder@imperial.ac.uk; b.pal@imperial.ac.uk).

C. Dufour is with Opal RT-Lab, Montreal, QC H3K 1G6, Canada (e-mail: christian.dufour@opal-rt.com).

P. Korba is with Asea Brown Boveri Switzerland, CH 5405 Baden, Switzerland (e-mail: petr.korba@ch.abb.com).

Digital Object Identifier 10.1109/TPWRS.2006.873020

TABLE I  
OPEN- AND CLOSED-LOOP SYSTEM DAMPINGS

Open Loop		Analytical Solution		LMI Comprime	
Damping ratio	Frequency (Hz)	Damping ratio	Frequency (Hz)	Damping ratio	Frequency (Hz)
0.0626	0.3013	0.1042	0.3941	0.1681	0.3913
0.0435	0.5080	0.0288	0.3968	0.1410	0.4926
0.0554	0.6232	0.0855	0.4989	0.1154	0.6344
		0.0812	0.5399		
		0.0560	0.6267		

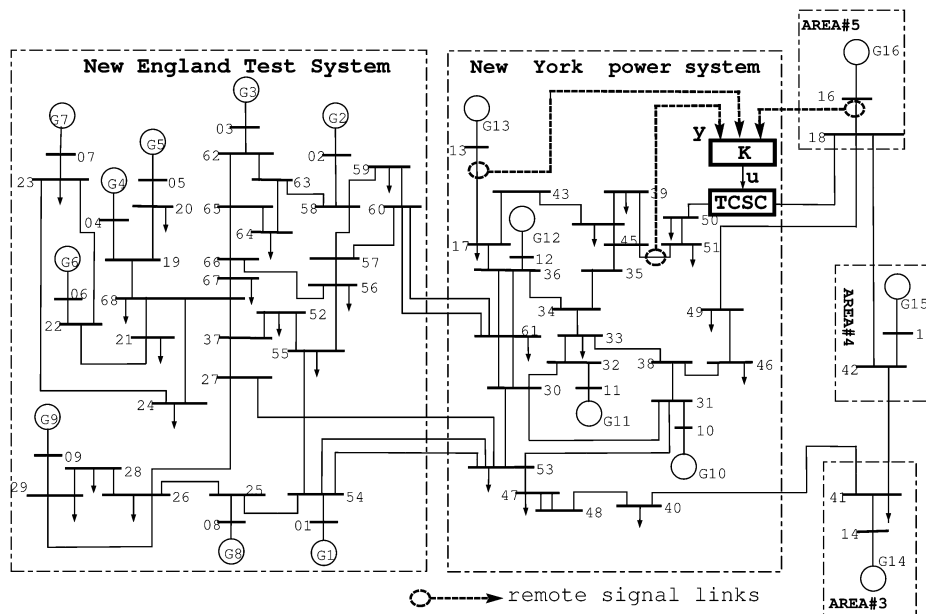


Fig. 1. Sixteen-machine five-area study system with TCSC.

implemented in a real-time platform. The performance of the controller is tested and compared with the simulated ones. The configurations of the hardware platforms and implementation test results are described in Sections V–VIII.

## II. CONTROLLER DESIGN APPROACH

Control design and performance validation in a 16-machine 68-bus power system model are explained and discussed in one of our recent papers [15]. The normalized coprime factorization approach for loop-shaping design was originally proposed by McFarlane and Glover [10]–[12]. The two-stage design procedure is based upon  $\mathcal{H}_\infty$  robust stabilization combined with classical loop-shaping. First, the open-loop plant is augmented by pre- and post-compensators to give a desired shape to the open-loop frequency response. Then the resulting shaped plant is robustly stabilized with respect to coprime factor uncertainties by solving the  $\mathcal{H}_\infty$  optimization problem. In [15], the standard normalized coprime factorization-based problem is converted into a generalized  $\mathcal{H}_\infty$  problem in the LMI framework with additional pole-placement constraints [17], [18]. The time-domain specifications in terms of minimum damping ratios (pole-placement) could not be considered explicitly in the design stage when the problem is solved analytically using standard normalized coprime factorization approach. Table I displays open-loop damping ratios of the critical inter-area modes and the closed-loop damping ratios obtained with both the approaches. It is seen

that two control modes with 0.1042 damping ratio at 0.3941 Hz and 0.0812 damping ratio at 0.5399 Hz are introduced. The inter-area mode damping ratios remain poor (0.0288 @ 0.3968 Hz and 0.0855 @ 0.4989 Hz) in analytical solution. Therefore, in this paper, the solution is obtained through an LMI optimization [17], [18] as it offers the flexibility to impose additional pole-placement constraints directly addressing the system damping. The pole placement objective is formulated in terms of LMI regions in the complex plane. There exists a general class of LMI regions for the above purpose, i.e., disks, conic sectors, vertical/horizontal strips, etc., or intersections of the above. A “conic sector” of inner angle  $\theta$  and apex at the origin is an appropriate LMI region for power system damping control application as it defines a minimum damping ratio for the dominant closed-loop poles. Details of the design methodology can be found in [15]. This paper implements that methodology in a dynamic power system emulator.

## III. STUDY SYSTEM

The control design and simplification exercises are carried out on a 16-machine, five-area study system model, as shown in Fig. 1. A thyristor controlled series capacitor (TCSC) is assumed installed in the system for strengthening the transmission corridor between NYPS and area #5. An eigenvalue analysis on the linearized model of the system revealed that the system had three critically damped inter-area modes ( $\lambda_i = -\sigma_i \pm j\omega_i$ ), as shown in Table II.

TABLE II  
INTER-AREA MODES OF THE STUDY SYSTEM

damping ratio ( $\zeta_i = -\frac{\sigma_i}{\sqrt{\sigma_i^2 + \omega_i^2}}$ )	frequency ( $f_i = \frac{\omega_i}{2\pi}$ (Hz))
0.0626	0.3913
0.0435	0.5080
0.0554	0.6232

The objective was to damp out these modes by designing a supplementary damping controller for the TCSC. Appropriate feedback stabilizing signals were chosen for each mode using the modal observability analysis (see [4] for methodology followed for signal selection).

#### IV. ROBUSTNESS VALIDATION BY LINEAR ANALYSIS

The damping action of the designed controller was examined under different types of disturbances in the system. These include changes in power flow levels over key transmission corridors, change of type of loads, etc. The damping ratios of the critical inter-area modes under these operating conditions are summarized in Fig. 2. In Fig. 2, CI, CP, and CC stand for constant impedance, constant power, and constant current type of loads, respectively. The damping ratios are found to be satisfactory in all the cases.

#### V. CHALLENGES OF REAL-TIME SIMULATION

Simulation has long been recognized as an important and necessary step in development, design, and testing of FACTS controller for mitigation of inter-area oscillations. Recent advances in both computing hardware, and sophisticated power system component modeling techniques have significantly increased application of real-time digital simulation in the power system industry.

##### A. Ability to Achieve a Small Time Step in a Large Inter-Connected Power System

Typically, a time step of about 1–10 ms is required to carry out an accurate simulation of power system dynamics if low-frequency electromechanical oscillations are concerned. The details of a set of differential algebraic equations describing the system are given in [19]. These equations could be solved with 1–10 ms time step without having the problem of numerical instability. Achieving such a time step can be problematic when trying to run the real-time simulation of a large inter-connected power system.

Such a small time step value is difficult to achieve with present computer technology because of inter-processors communication latency. However, it was demonstrated that off-the-shelf PC-based simulators like RT-LAB can achieve a time step value below 10 ms for systems of moderate size, such as 50–100 buses and up to 50 generators.

##### B. Scalability

A real-time simulator should be scalable in terms of computational power to enable the simulation of larger power systems as these are needed to analyze the interactions between several control systems and the power system itself. The simulator

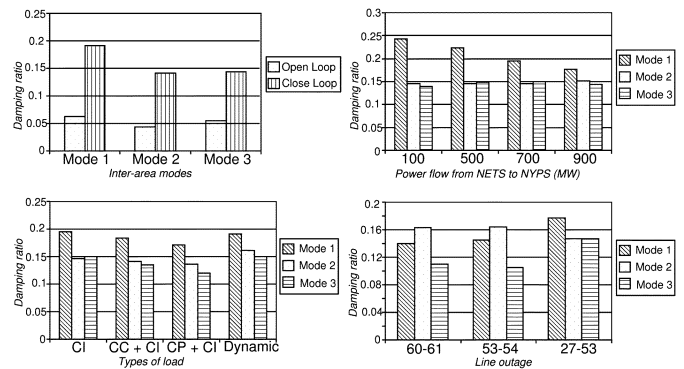


Fig. 2. Robustness validation through damping ratio.

scalability is achieved by distributing the simulation execution over several processors as the simulated network becomes more complex. This is achieved by breaking up the network into several linked subsystem, taking advantage of slowly varying state variables. However, special care must be taken in the selection of the inter-processor communication system to prevent excessive communication delays, which limit the minimum time step achievable.

#### VI. IMPLEMENTATION IN REAL-TIME PLATFORM

One of the most significant disadvantages of software simulations relates to the speed at which they operate. Unlike analogue simulator that operates in real time, most digital simulation systems operate in nonreal time. Real-time operation implies that an event in the system that lasts for 1 s can be simulated on the simulator exactly in 1 s. Any external hardware could be connected with system simulated in real time with in built DAC/ADC modules. Therefore, the controller under test whether implemented in a low-cost dedicated micro controller or in analogue circuitry could be interfaced with the real-time digital simulator. We have developed a real-time simulation platform that is used to simulate the dynamic behavior power system model for testing a FACTS controller as mentioned earlier.

#### VII. RT-LAB REAL-TIME STATION AND RAPID PROTOTYPING CONTROLLER

##### A. RT-LAB Real-Time Station

A schematic view of the RT-LAB real-time station is depicted in Fig. 3. The RTS is a PC running on real-time operating system RedHawk RT-Linux. It has dual-Xeon processor of 3.2 GHz. Both the processors share a common memory, as shown in Fig. 3.

The separation of the tasks involved in simulating the power system dynamic behavior is depicted in Fig. 3. The computational tasks are distributed as follows: CPU1 of the dual-CPU processor runs the differential equations describing the dynamic behavior of the generators, associated excitation systems, and the FACTS device (TCSC, in this case). The CPU2 simultaneously solves the network equations to connect the generators with the network. The most computationally expensive task is to solve the set of network equations to calculate the complex

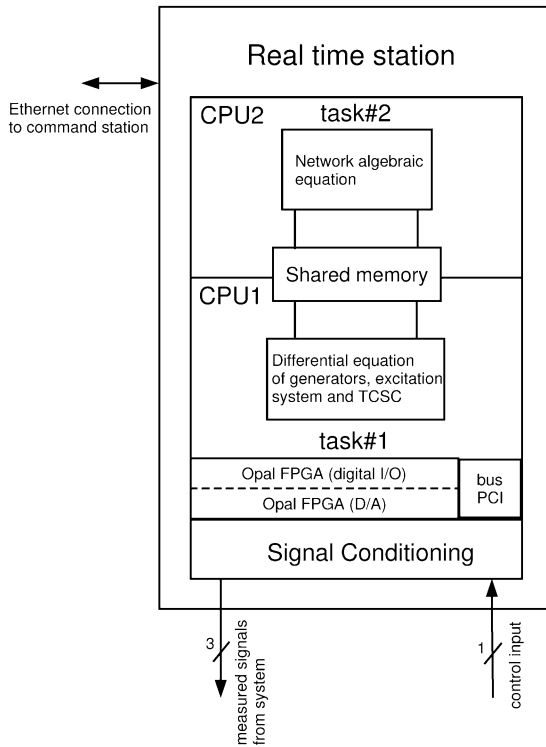


Fig. 3. Schematic diagram of RTS with system task separation.

bus voltages from the admittance matrix and the set of complex bus currents. The inversion of the admittance matrix is avoided by using LU factorization. The LU factors of the admittance matrix are pre-computed and stored. Due to the change in series compensation of the TCSC, the admittance matrix is required to be updated dynamically. An optimal ordering of the TCSC bus is done to keep the computational burden minimal. In the current application, the CPU in charge of solving the differential equations associated with the generators, excitation system, and TCSC also controls the field programmable gate arrays (FPGA) I/O card that sends the measured signals from the plant and reads the control signal generated by the rapid prototyping controller (RPC). The digital signal generation and sampling are both obtained using 10-ns resolution. The FPGA card, built around the Xilinx Virtex-II Pro, also controls fast 16-bit D/A and A/D converters. The sampling time used in the real-time simulation is 1 ms. CPU1 takes around 300–450  $\mu\text{s}$  to solve the differential equations. The computational time required by CPU2 in solving the algebraic equations simultaneously takes nearly 800  $\mu\text{s}$ . Therefore, no over-runs are detected during the real-time operation. The RTS is a multi-applications real-time platform suitable for hosting a wide variety of dynamic applications and, unlike other real-time simulation environments, is not confined only to power systems. Bearing in mind the cost associated with this state-of-the-art technology, and its ability to support a wide variety of dynamical systems applications, over a variety of disciplines, it makes the facility a very useful laboratory resource.

### B. RT-LAB RPC

RPC is a PC that has a Pentium 4 processor running at 3.2 GHz under RedHawk RT-Linux operating system with capability of handling I/O interaction in real time. Once the con-

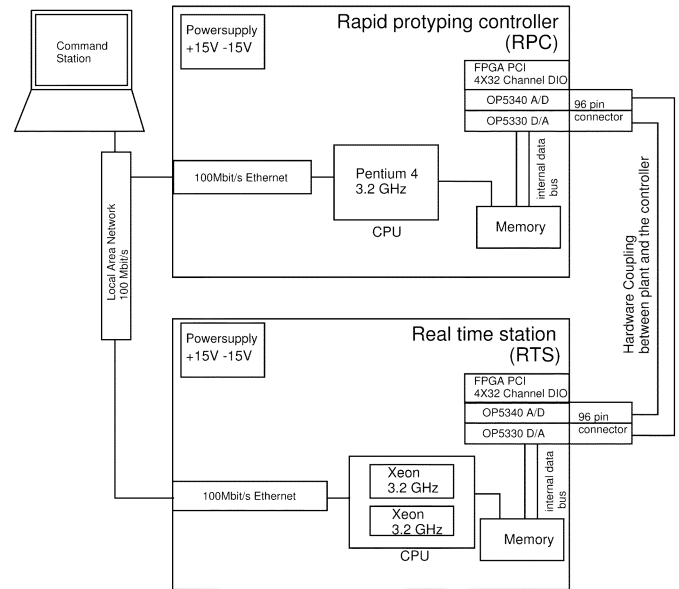


Fig. 4. Schematic diagram of RTS and RPC.

troller is designed and realized in its state-space form, it can be implemented in the RPC. Computational time for the RPC to calculate control signal is about 60  $\mu\text{s}$ , which is well within the sampling period. In practical situations, the controller could also be implemented in any dedicated low-cost micro controller. Internal architecture and the I/O interfacing of the RPC and the RTS are almost identical. The efficacy of the designed robust controller is proved in real time by implementing it on the RPC.

### C. Hardware-in-Loop (HIL) Configuration of RTS and RPC

A Windows host command station is used to set up various test scenarios and evaluate controller performance for different system disturbances, operating conditions, and topologies. The host command station and both the real-time digital simulators interact between themselves through 100 Mbit/s ethernet connection. The schematic diagrams of the RTS and the RPC are shown in Fig. 4. If necessary, the computational tasks can be distributed across several PCs to decrease the simulation time step or to simulate more complex systems. Inter-computer communication systems supported by RT-LAB are FireWire 800-Mbits/s as well as SignalWire, which is an FPGA-based fast serial communication link capable of delivering up to 1.25 Gbit/s transfer rates, with a latency of 200 ns.

In RTS platform, the input model is developed in MATLAB Simulink. A graphical user interface, called RT-lab main control for managing the communication between the RTS and the command station, is available. Real-time workshop (RTW) of MATLAB interfaces Simulink and this hardware platform. The RT-lab main control is used to build real-time code and to download and execute this code on Xeon processor of RTS through ethernet link. Any signal from the model can be brought outside through built-in DAC, and any physical signal can be fed back to the system using in built ADC.

Robust damping controller is a three-input, one-output controller implemented in RPC. The same RT-lab main control is used to generate code for the controller and to download it to

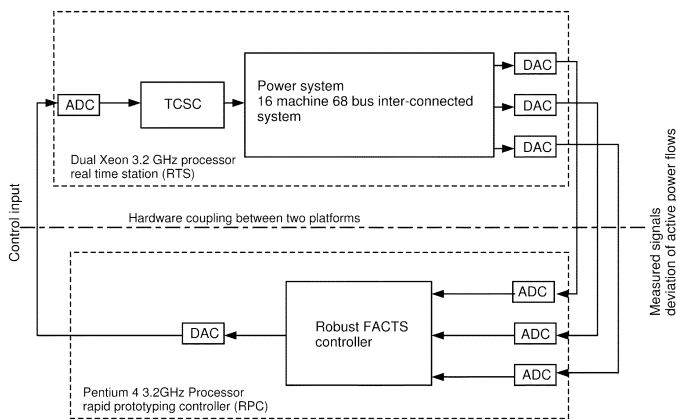


Fig. 5. Closed-loop configuration of RTS and RPC.

RPC for real-time execution through ethernet link. The inputs to this controller are a deviation in the active power flow through the transmission line connecting buses #51–#45, #18–#16, and #13–#17. These signals are generated in the RTS and are interfaced with the controller through on-board DACs of RTS, as shown in Fig. 5. The control signal is computed by the RPC at every sampling instant and fed back to the simulated power system via a DAC-ADC combination, as shown in Fig. 5.

### VIII. EXPERIMENTAL RESULTS

The performance of the designed controller implemented on RPC has been evaluated for various operating conditions, using the emulated power system on RTS. The deviation in active power flow through transmission line from RTS was sampled and fed to the controller. The control signal is fed back to the TCSC.

#### A. Validity Check

The validity of implementation of the nonlinear power system model on the RTS is first established by a number of identical tests performed on the RTS and the same system modeled using MATLAB-Simulink on a PC. A representative set of results are shown in Figs. 6 and 7. A three-phase-to-ground fault is created at 1 s into the simulation at bus #27 and the fault is cleared after 80 ms, followed by opening of one of the tie-lines connecting buses #27 and #53. Fig. 6 shows deviation in active power flow in transmission line connecting bus #51–#45 in MATLAB-Simulink, and Fig. 7 shows the same while the system is implemented in RTS. The dynamic behavior of the study system is thus emulated in real time using the RTS with reasonable accuracy.

#### B. Case Studies

One of the severe disturbances stimulating poorly damped inter-area oscillations is a three-phase fault in one of the key transmission corridors. For temporary faults, the circuit breaker “auto-recloses” and normal operation is restored; otherwise, one or two lines might have to be taken out. There might be other types of disturbances in the system like change of load characteristics, sudden change in power flow, etc. which are less severe compared to faults and are not considered here.

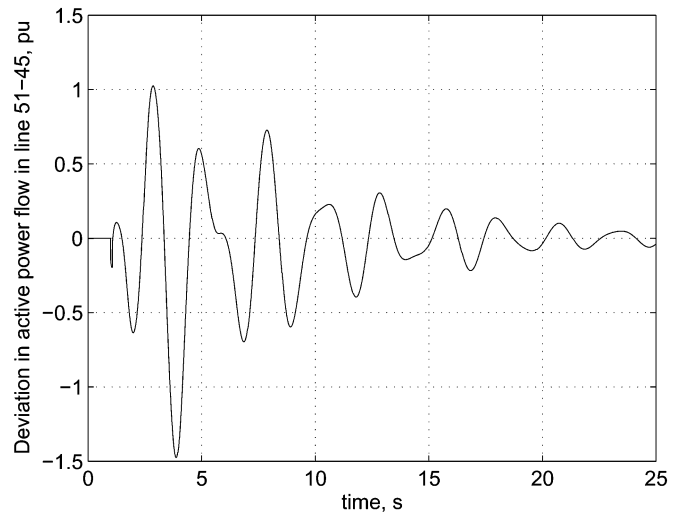


Fig. 6. Dynamic response of the system, MATLAB Simulink Environment.

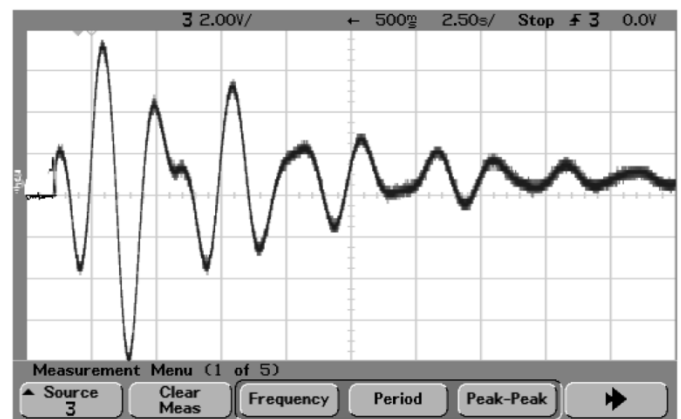


Fig. 7. Dynamic response of the system, real-time station, dual Xeon Processor in real time.

Simulations were carried out to evaluate the performance and robustness of the designed controller corresponding to some of the probable fault scenarios in the NETS and NYPS inter-connection. There are three transmission corridors between NETS and NYPS connecting buses #60–#61, #53–#54, and #27–#53, respectively. Corridors connecting buses #60–#61 and #53–#54 consists of two tie-lines, and the corridor connecting buses #27–#53 consists of one tie line. The outage of one of these lines weakens the transfer capacity of the inter-connection considerably. The following disturbances were considered for simulation. A three-phase solid fault for 80 ms (five cycles)

- 1) at bus #60 followed by auto-reclosing of the circuit breaker;
- 2) at bus #53 followed by outage of one of the tie-lines connecting buses #53–#54;
- 3) at bus #53 followed by outage of the tie-line connecting buses #27–#53;
- 4) at bus #60 followed by outage of one of the tie-lines connecting buses #60–#61.

The designed controller is supposed to settle the inter-area oscillations within 12–15 s following any of the disturbances. Moreover, it should be able to achieve this following any of the above disturbances (robustness), although the design is based on a

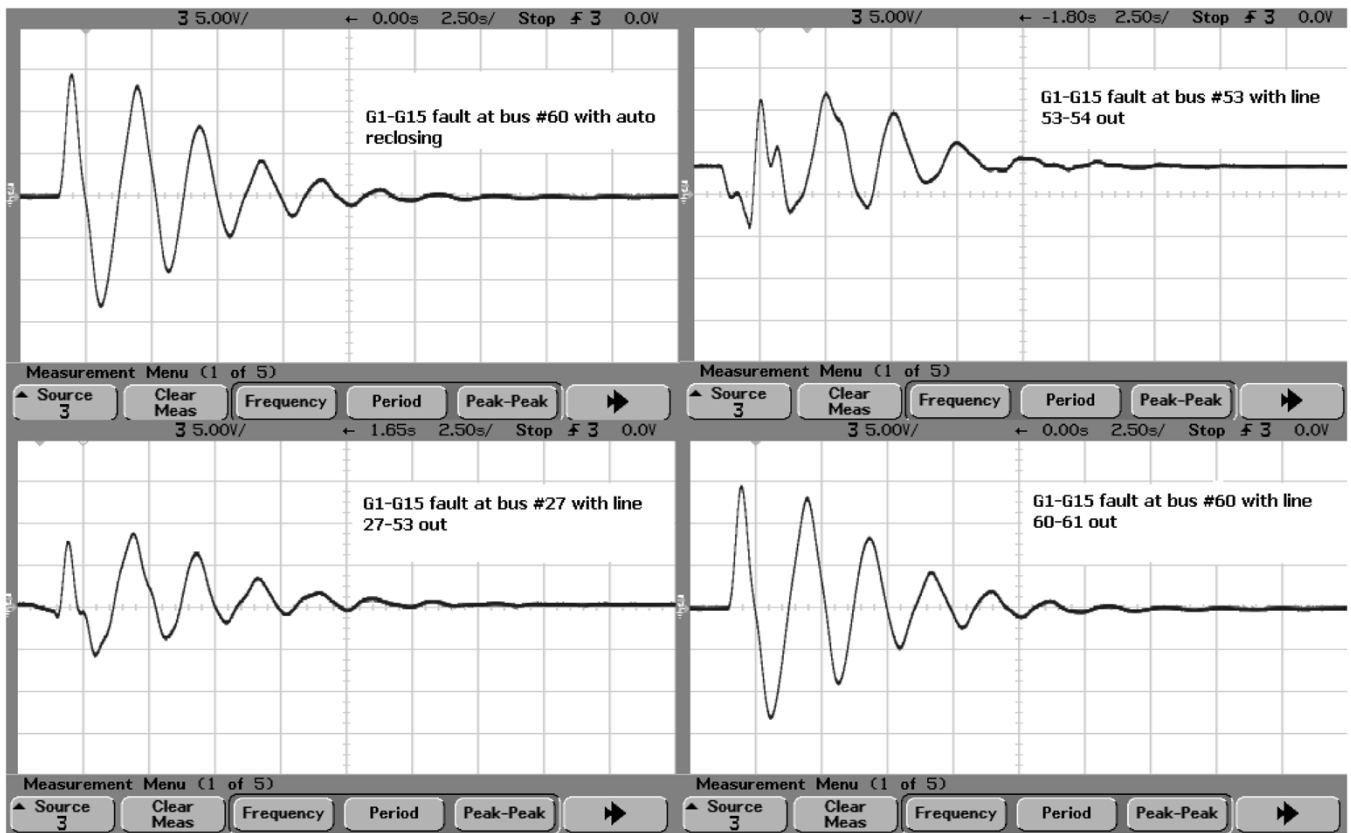


Fig. 8. Response of the system observed in relative angular separation between generators 1 and 15 for faults in various tie-lines.

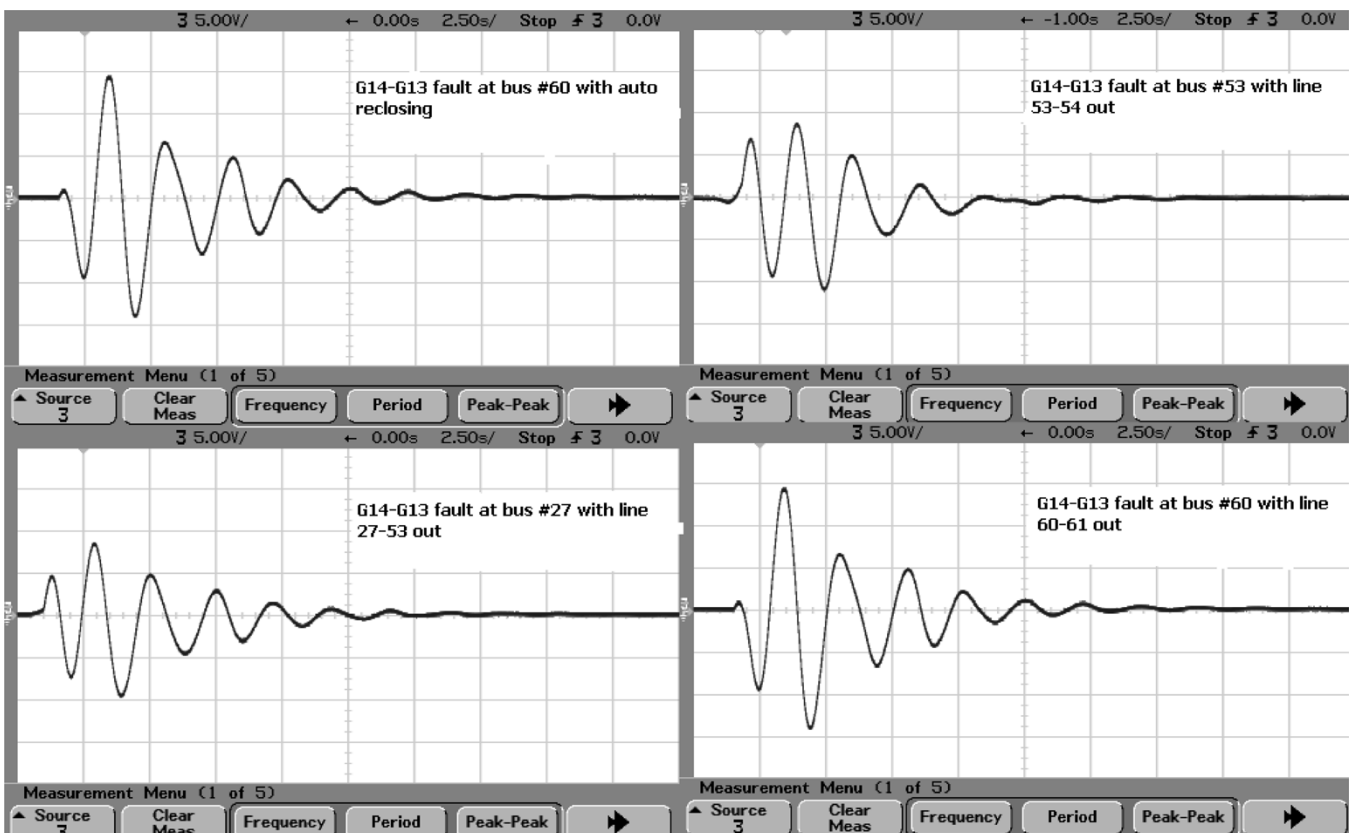


Fig. 9. Response of the system observed in relative angular separation between generators 14 and 13 for faults in various tie-lines.

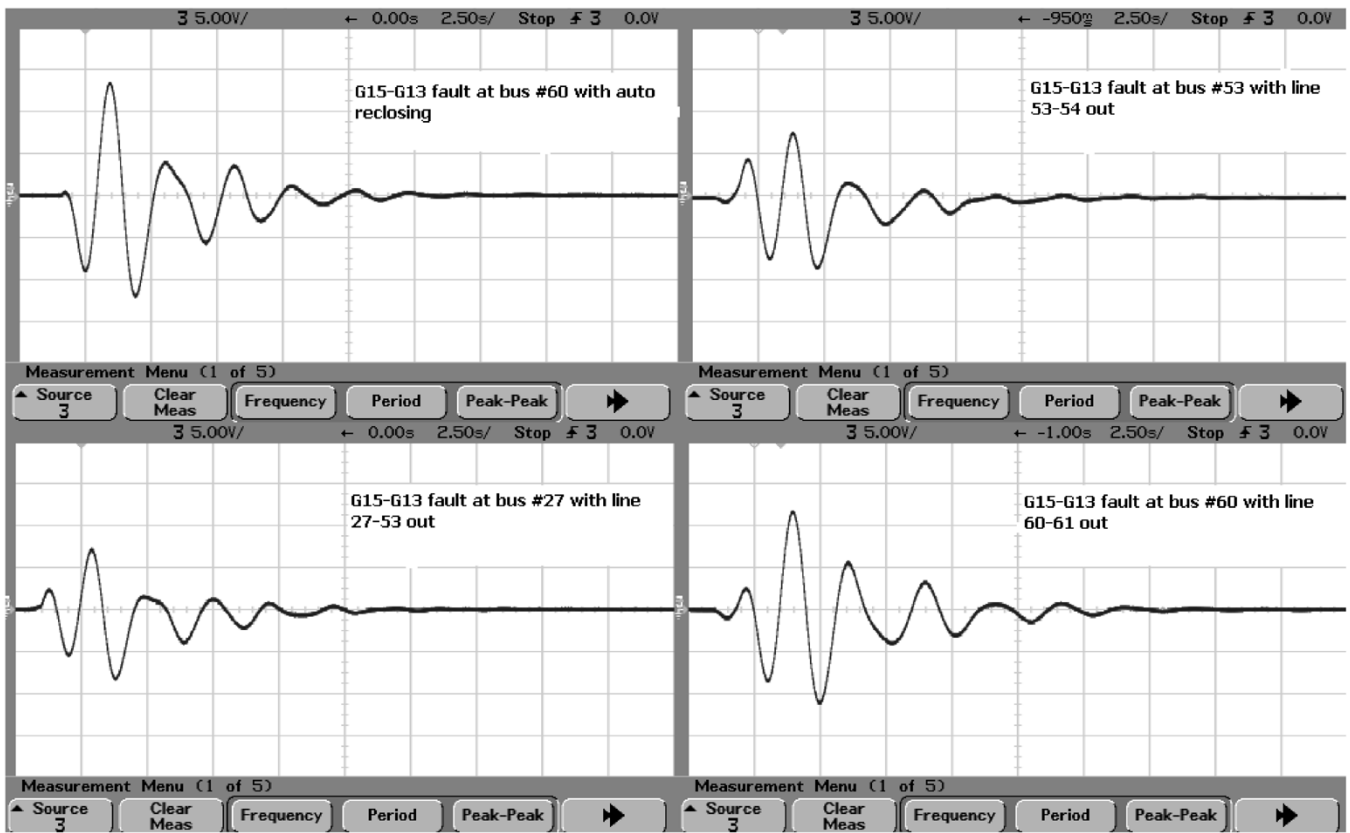


Fig. 10. Response of the system observed in relative angular separation between generators 15 and 13 for faults in various tie-lines.

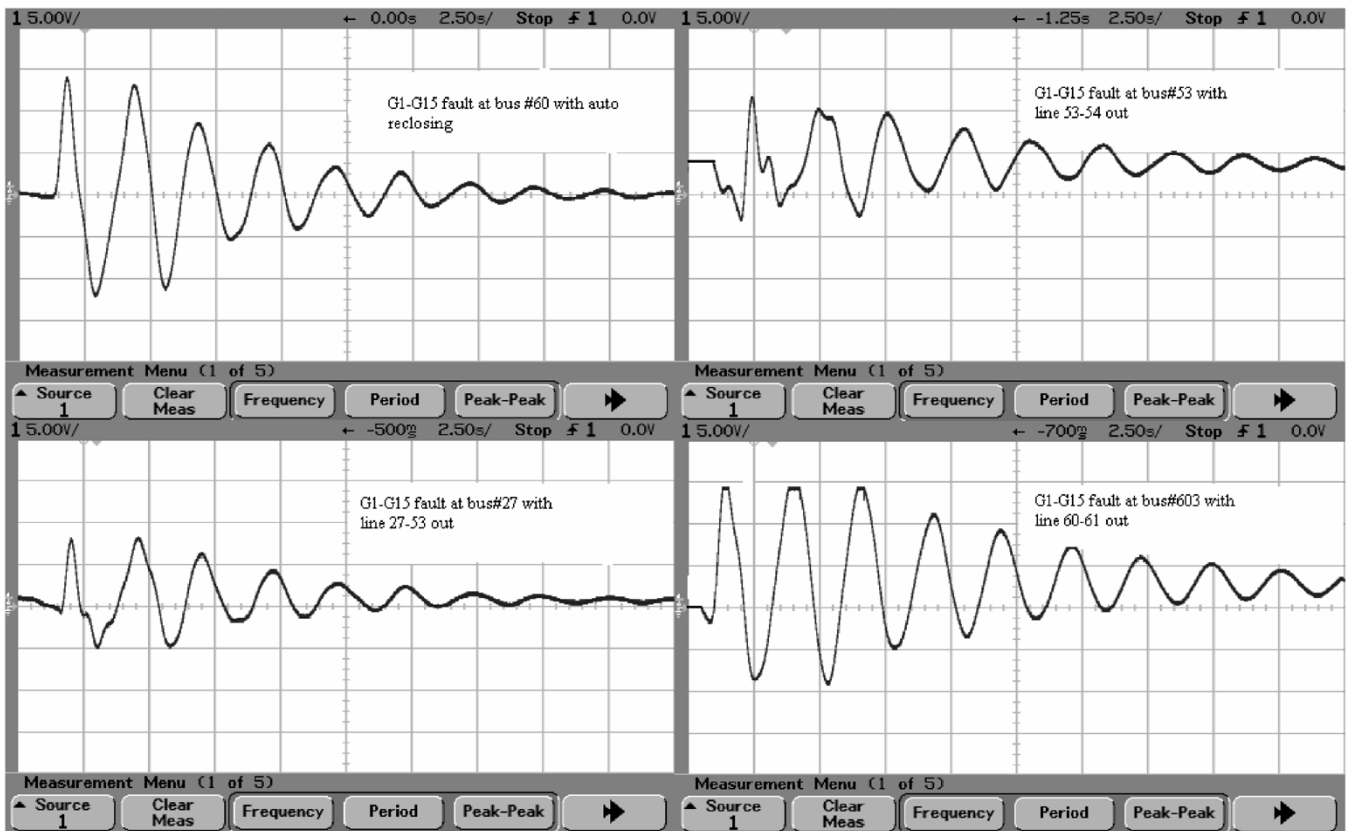


Fig. 11. Response of the system with controller designed based on analytical solution (relative angular separation between generators 1 and 15).

nominal operating condition (no outage). The relative angular separations of the generators located in different geographical areas are given in Figs. 8–10. The designed robust FACTS controller is shown to be physically implementable with a performance, which is maintained over a wide range of operating conditions. In Figs. 8–10, time per division is 2.5 s. To compare the performance of controllers designed based on analytical solution and controller synthesized by numerical solution using LMI, the same set of tests were carried out. Fig. 11 shows the closed-loop response with controller designed based on analytical solution. The damping performance of the analytically designed controller is not satisfactory, as was observed from linear analysis (see Table II).

## IX. CONCLUSION

This paper has demonstrated the application of the normalized  $\mathcal{H}_\infty$  loop-shaping technique for the design of damping controllers in the LMI framework. The first step in this design approach is to pre- and post-compensate the linearized model of the power system using loop-shaping technique. The problem of robust stabilization of a normalized coprime factor plant description was translated into a generalized  $\mathcal{H}_\infty$  problem. The solution was sought numerically using LMIs with additional pole-placement constraints. An important contribution of this paper is the realization of a multi-machine power system model which is capable of providing results in real time on a commercially available RTS. The designed control algorithm is implemented in a rapid prototyping controller, and the coupling between RTS and RPC is done through DAC/ADC module in analogue domain. The real-time multi-machine model has opened the door to many possible application areas, including the provision of a flexible test bench for the development and testing of physical controllers and network compensators.

## REFERENCES

- [1] J. Paserba, "Analysis and control of power system oscillation," *CIGRE Special Publ. 38.01.07, Tech. Brochure 111*, 1996.
- [2] N. Hingorani and L. Gyugyi, *Understanding FACTS*. Piscataway, NJ: IEEE Press, 2000.
- [3] B. Chaudhuri, B. Pal, A. C. Zolotas, I. M. Jaimoukha, and T. C. Green, "Mixed-sensitivity approach to  $H_\infty$  control of power system oscillations employing multiple facts devices," *IEEE Trans. Power Syst.*, vol. 18, no. 3, pp. 1149–1156, Aug. 2003.
- [4] B. Chaudhuri and B. Pal, "Robust damping of multiple swing modes employing global stabilizing signals with a TCSC," *IEEE Trans. Power Syst.*, vol. 19, no. 1, pp. 499–506, Feb. 2004.
- [5] M. Klein, L. Le, G. Rogers, S. Farrokpay, and N. Balu, " $H_\infty$  damping controller design in large power system," *IEEE Trans. Power Syst.*, vol. 10, no. 1, pp. 158–166, Feb. 1995.
- [6] G. Taranto and J. Chow, "A robust frequency domain optimization technique for tuning series compensation damping controllers," *IEEE Trans. Power Syst.*, vol. 10, no. 3, pp. 1219–1225, Aug. 1995.
- [7] Q. Zhao and J. Jiang, "Robust SVC controller design for improving power system damping," *IEEE Trans. Power Syst.*, vol. 10, no. 4, pp. 1927–1932, Nov. 1995.
- [8] M. Djukanovic, M. Khammash, and V. Vittal, "Sequential synthesis of structured singular value based decentralized controllers in power systems," *IEEE Trans. Power Syst.*, vol. 14, no. 2, pp. 635–641, May 1999.
- [9] S. Chen and O. Malik, "Power system stabilizer design using  $\mu$  synthesis," *IEEE Trans. Energy Convers.*, vol. 10, no. 1, pp. 175–181, Mar. 1995.

- [10] D. McFarlane and K. Glover, *Robust Controller Design Using Normalized Coprime Factor Plant Descriptions*. ser. Lecture Notes in Control and Information Sciences, M. Thoma and A. Wyner, Eds. Berlin, Germany: Springer-Verlag, 1990.
- [11] —, "A loop shaping design procedure using  $H_\infty$  synthesis," *IEEE Trans. Autom. Control*, vol. 37, no. 6, pp. 759–769, Jun. 1992.
- [12] K. Glover and D. McFarlane, "Robust stabilization of normalized coprime factor plant descriptions with  $H_\infty$ -bounded uncertainty," *IEEE Trans. Autom. Control*, vol. 34, no. 8, pp. 821–830, Aug. 1989.
- [13] C. Zhu, M. Khammash, V. Vittal, and W. Qiu, "Robust power system stabilizer design using  $H_\infty$  loop shaping approach," *IEEE Trans. Power Syst.*, vol. 18, no. 2, pp. 810–818, May 2003.
- [14] M. Farsangi, Y. Song, W. Fang, and X. Wang, "Robust facts control design using  $H_\infty$  loop-shaping method," *Proc. Inst. Elect. Eng., Gen., Transm., Distrib.*, vol. 149, no. 3, pp. 352–357, May 2002.
- [15] R. Majumder, B. Chaudhuri, H. El-Zobaidi, B. Pal, and I. M. Jaimoukha, "LMI approach to normalized h-infinity loop-shaping design of power system damping controllers," *Proc. Inst. Elect. Eng., Gener., Transm., Distrib.*, vol. 152, no. 6, pp. 952–960, Nov. 2005.
- [16] P. Gahinet, A. Nemirovski, A. Laub, and M. Chilali, *LMI Control Toolbox for use with Matlab*. Boston, MA: Math Works, 1995.
- [17] M. Chilali and P. Gahinet, "Multi-objective output feedback control via LMI optimization," *IEEE Trans. Autom. Control*, vol. 42, no. 7, pp. 896–911, Jul. 1997.
- [18] C. Scherer, P. Gahinet, and M. Chilali, " $H_\infty$  design with pole placement constraints: An LMI approach," *IEEE Trans. Autom. Control*, vol. 41, no. 3, pp. 358–367, Mar. 1996.
- [19] B. Chaudhuri, R. Majumder, and B. Pal, "Application of multiple-model adaptive control strategy for robust damping of interarea oscillations in power system," *IEEE Trans. Control Syst. Technol.*, vol. 12, no. 5, pp. 727–736, Sep. 2004.

**Rajat Majumder** (S'03) received the B.E.E. (Hons) degree from Jadavpur University, Calcutta, India, and the M.Sc. (Engg.) degree from the Indian Institute of Science, Bangalore, India, in 2000 and 2003, respectively. He is currently working toward the Ph.D. degree in the Control and Power Group, Imperial College London, London, U.K.

**Bikash C. Pal** (SM'02) received the B.E.E. (Hons) and M.E. degrees from Jadavpur University, Calcutta, India, and the Indian Institute of Science, Bangalore, India, in 1990 and 1992, respectively. He received the Ph.D. degree from Imperial College London, London, U.K., in 1999.

He is presently a Senior Lecturer in the Department of Electrical and Electronic Engineering, Imperial College London. His research interest is in the area of power system dynamics and FACTS controllers.

**Christian Dufour** (M'96) received the B.S. degree in electrical engineering, the M.S. degree, and the Ph.D. degree in fiber optics from Laval University, Quebec City, QC, Canada, in 1990, 1994, and 2000, respectively.

He worked as Software Developer for the Institut de Recherche d'Hydro-Quebec (IREQ) on HYPERSIM, Hydro-Quebec's real-time numerical power system simulator and the Power System Blockset first release. Presently, he is in Opal-RT, Montreal, QC, Canada, as a Simulation Software Specialist, where he is involved in the design and development of real-time applications in the field of electrical systems and drives. He is the main developer of ARTEMIS, which is based on his Ph.D. thesis.

**Petr Korba** received the M.Sc. degree in electrical engineering from the Czech Technical University, Prague, Czech Republic, and the Ph.D. degree (with honors) from the University of Duisburg, Duisburg, Germany, in 1995 and 2000, respectively.

He was a Visiting Scientist in control engineering at the University of Technology in Delft, The Netherlands, in 1998 and at the University of Manchester Institute of Science and Technology (UMIST), Manchester, U.K., in 1999. He worked as a Research Associate and Member of Staff at UMIST, Control Systems Centre, until 2001. He is currently with Asea Brown Boveri (ABB) Switzerland, Ltd., Corporate Research. His research interests include model-based fuzzy control, gain-scheduling, and robust control and their applications.